Devoting turbidity measurements via absorptiometry: glutathione determination

Haifa Rasool Salim and Naser A. Naser*

Department of Chemistry, Faculty of Science, University of Kufa, P.O. Box (21), Najaf Governorate, Iraq.

Haifa4144@gmail.com and nasir.almutawiri@uokufa.edu.iq

Abstract

The study included estimation of glutathione (GSH) as an important biomarker using turbidimetric method based on reaction of GSH with Ce(IV) in acidic medium to form turbid solution. More than twenty metal ions were used to test their interaction with GSH in acidic medium, it was obtained that only Ce(IV) forms turbid product. Instead of using turbidimeter to conduct measurements, a single beam spectrophotometer was used for this purpose. The measurements were studied at three wavelengths via 500, 700 and 900nm, but a near infrared wavelength, i.e. 900nm, shows the best results. In addition, the effect of temperature, time, type of acid, sequence addition as an optimum conditions required for the product to form were studied. Then the effect of the interferences was studied at two concentrations. A calibration curve in $\mu g.mL^{-1}$ was constructed and its trending lies on points of concentrations ranged from 20 to 180$\mu g.mL^{-1}$ with a correlation coefficient of 0.9994, and detection limit of 0.0005 $\mu g.mL^{-1}$ and slope is (0.0014). The analytical method was applied on samples of human blood serum. The obtained results were compared with the results of the referenced (kit) method. The results obtained by the method followed, some of them were close and the others were far.

Keywords: glutathione; turbidity; determination; absorptiometry

1. Introduction

Glutathione (GSH) is the most prevalent thiol-containing low-molecular-mass sulfhydryl group (-SH) and a non-proteinogenic tripeptide. Its chemical name is γ-L-glutamyl-L-cysteyl-glycine (1). GSH is present in mammalian cells at concentrations ranging from 1 to 10 mmol l^{-1} (2) but in serum and plasma, it is reduced to 150-200 μM and 1-6 μM, respectively (3). Almost all of the body's cells contain GSH(4),

which is widely presents in a variety of essential tissues and organs for example liver, kidney and blood, where the liver and kidneys are the major synthetic, metabolic, and excretory organs for GSH (5), GSH is synthesized from glutamate, glycine, and cysteine (6), with a γ-carboxyl linkage between cysteine and glutamate of GSH that, unlike the typical -carboxyl group, is only vulnerable to hydrolysis by γ-glutamyltranspeptidase (7). This gives resistance to intracellular degradation (8). The active reducing group in GSH's structure, sulfydryl (-SH), is rapidly oxidized and dehydrogenated. Glutathione reductase (GSH-R) may catalyze the conversion of GSSG to GSH using nicotinamide adenine dinucleotide phosphate (NADPH), whereas glutathione peroxidase (GSH-Px) can catalyze the conversion of GSH to GSSG. The major active group in GSSG is the disulfide bond (-SS-) (9,10). To describe the redox and metabolic status of biological systems in vivo and in vitro, measurements of glutathione (GSH), glutathione disulfide (GSSG), and related intermediates are required(11).

Increased oxidative stress causes an increase in GSSG and GSH conjugates with electrophiles, which lowers intracellular GSH levels (12). Oxidative damage is known to have a role in the initiation and development of many disease states and GSH deficiency contributes to oxidative damage (13)(14). On the other hand, as seen in many different kinds of cancer cells, increased GSH levels typically confer resistance to oxidative stress(15)(16) . The accurate measurement of GSH and GSSG in blood and tissues in absolute and ratiometric terms is therefore considered a putative tool in oxidative stress investigations (8). For detecting glutathione, a number of techniques based on fluorescence(17), colorimetric detection (18), mass spectroscopy(19) and Liquid Chromotagraphy (20) have been published.

2. Materials and methods

2.1 Instruments

The UV-visible spectra were recorded using quartz cells of 1 on an ultraviolet–visible spectrophotometer (T80- PG Instruments Ltd., UK). The measurements of pH were achieved using a calibrated pH meter (WTW 340i, Germany. Using Stapt-1000 Linseis).

2.2 Materials

All solutions of chemicals used were prepared in water and were all of the analytical reagent grade. Glutathione was supplied by Failing. Acids like HCl, HNO_3, H_2SO_4 were supplied by BDH, RDH and Merck respectively.

2.3 Preliminary Tests of glutathione with metal ions

Many metal ions were examined with glutathione solution. Metals are; Ag^{+}, Bi^{3+}, Cd^{2+}, Hg^{2+}, MoO_4^{2-}, Co^{2+}, Cu^{2+}, Pb^{2+}, Fe^{2+}, Zn^{2+}, Ce^{4+}, Sn^{2+}, Mg^{2+}, Ni^{2+}, K^{+}, La^{3+}, Mn^{2+}, MnO_4^{2-}, Li^{+}, Cr^{3}. Solutions were mixed and tested at acidic and basic media. From these compounds, only cerium ion shows its ability to causes turbid solution in acidic medium.

2.4 Measurements of glutathione in real samples(in serum)

2.4.1 Participants

Participants are individuals that have in some form contributed to the development on the GSH spectrophotometric assay.

Eighty volunteers were participated in the current study. Volunteers are students of 2nd year. They were with no chronic disease. They were 20 – 24 years old (40 male and 40 female).

For the purposes of our study human biological samples such as blood and serum were needed to test the capability of GSH assay.

Human blood and serum were chosen as there are easy samples to collect from volunteers.

These samples were collected as de-identified pathologic discard whole blood and serum samples.

2*.4.2 Protein precipitation*

The analysis of small molecules in biological samples is frequently hindered by the presence of protein and various enzyme activities. Many bioassays require removal of protein from samples prior to analysis. There are many different procedures for this purpose. Protein precipitation method using organic solvents was adopted in the current study.

3. Results and discussion

3.1 GSH – Ce (IV) reaction, turbid product

Among the ions that were tested with glutathione, it was found that the cerium(IV) was the single ion that showed turbidity in the presence of acidic medium. This characteristic and chemical reaction have been exploited as a method for the study and quantification of glutathione. The chemical structure of the GSH binding to the metal in turbid product was identified by the Infra-red and UV-visible spectroscopy, Figures 1 and 2.

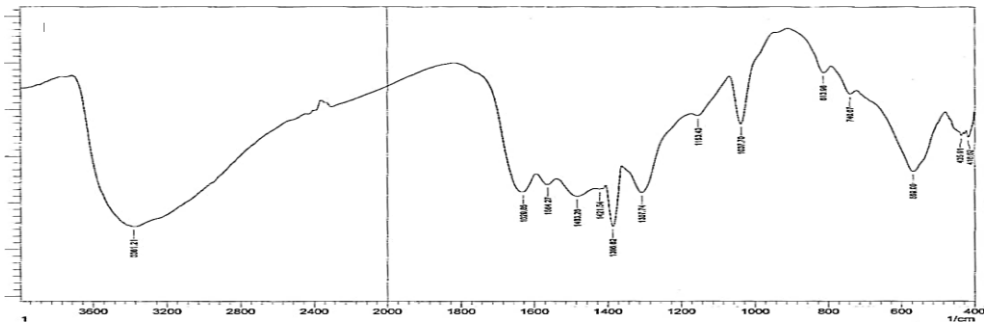

Figure 1: FTIR Spectrum of the turbide product.

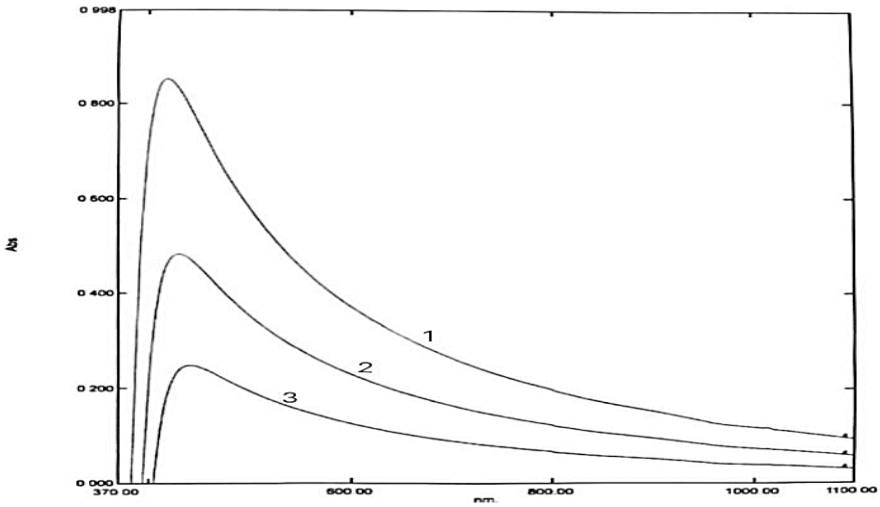

Figure 2: UV-Vis. Spectrum of the turbide product at three concentrations, 1: more concentrated and 3: the diluted solution.

3.2 Measuring turbidity on a spectrophotometer

Decades ago, it was proposed that spectrophotometers can be used to measure not just
the absorbance of absorbing samples, but also the turbidity of non-absorbing samples. This is because while spectrophotometers report an `absorbance' A, the quantity that

is actually measured is how much light does not make it through the sample towards a detector situated opposite from the light source.

Thus a typical spectrophotomer reports an `absorbance' as follows:

$$\text{Abs} = -\log_{10}(I=I_0) = \epsilon = A + \tau \qquad \text{---------- (1)}$$

where I_0 is the incident light intensity, I is the intensity of light that enters the detector,

τ is the extinction owing to scattering. It is assumed that no light is scattered into the detector. This assumption was revisited in the section examining the effects of scattering

towards the detector.

For absorbing samples that have insignificant light scattering ($\tau = 0$), the measured quantity ϵ equals a true absorbance A and the concentration of a sample can be determined

by using $A = \epsilon_A cl$, otherwise known as the Beer-Lambert law. Here ϵ_A is the molar ab-

sorption coefficient ($[\epsilon_A] = M^{-1}\ cm^{-1}$), c is the concentration of the absorbing molecule ($[c]$

moles/L = M) and l is path length (usually through a cuvette, $l \sim 1$ cm).

When describing non-absorbing samples, the total attenuation of light after it passes through a sample is usually described by a turbidity or optical depth τ:

$$\tau = -\ln(I=I_0) = \sigma_{sca} Nl \qquad \text{---------- (2)}$$

assuming the fraction of light scattered in the direction of the detector is insignificant. σsca

is the scattering cross section per scatterer (e.g. a vesicle, $[\sigma_{sca}] = m^2$), and N is the number density of scatterers ($[N] = m^{-3}$). By equations 1 and 2, the turbidity of a non-absorbing

sample ($A = 0$) can be measured on a spectrophotometer: the `absorption' ϵ measured on

spectrophotometers is in fact linearly proportional to the turbidity $\tau \sim 2.3\epsilon = 2.3\ \tau$.

3.3 Experiments for focusing the best conditions for GSH assessment

In order to obtin the reaction with less amounts of participating materials as well as to more stable product the following experiments were conducted:

3.3.1 Optimization of concentrations during GSH assay

In this study, too many experiments were conducted in order to obtain the optimum concentrations for the participated materials in GSH assessment.

Table 1 shows results of reacting different concentrations of Ce(IV) solution with GSH(at 0.005 M) using three drops of concentrated HCl at three wavelengths.

Table 1: Effect of different concentrations of Ce(IV) on GSH assessment at three wavelengths.

Ce(IV), mol/Lit	λ = 500nm	λ = 700nm	λ = 900nm
0.001	0.070	0.042	0.022
0.003	0.201	0.105	0.063
0.005	0.408	0.216	0.099
0.007	0.393	0.215	0.097
0.01	1.135	0.650	0.385

3.3.2 The effect of the type of acid used

Different acids were used for this experiment. Acids; acetic acid, sulphuric acid, nitric acid and hydrochloric acid were used. Further, the concentrations used for the ceric ammonium nitrate and GSH were 0.01 and 0.005 M, respectively. Table 2 shows results of the best acid for GSH assay at three wavelengths.

Table 2: Acids used for selecting the best acid for GSH assay

Acid	λ = 500nm	λ = 700nm	λ = 900nm
HNO_3	0.332	0.228	0.123
HCl	0.712	0.269	0.159
CH_3COOH	0.016	0.161	0.009
H_2SO_4	0.520	0.149	0.109

It is obvious from results showed in table 2 that the optimization yields a greater absorbance obtained when HCl is employed.

3.3.3 Temperature effect on the turbid product

At different temperatures that were taken within the range from 0 to 60 °C, the effect of temperature on the speed of formation and stability of the turbid product was investigated,

Table 3 shows results for the effect of temperature on turbid product formation at two wavelengths

As in the previous study, conditions apllied for this procedure were 0.01 M of ceric ammonium nitrate solution and 0.005 M of GSH using three drops of concentrated HCl. However, eleven exerpiments at different temperatures were acheieved.

Table 3: The effect of Temperature on the turbid product.

T (℃)	λ = 500nm	λ = 700nm	λ = 900nm
0	0.610	0.274	0.138
10	0.640	0.245	0.209
20	0.697	0.265	0.277
25	0.757	0.329	0.289
30	0.791	0.382	0.281
35	0.686	0.347	0.271
40	0.655	0.348	0.211
45	0.602	0.315	0.191
50	0.570	0.279	0.187
55	0.543	0.268	0.166
60	0.488	0.254	0.163

3.3.4 Addition sequence effect

The sequence of addition to the components of the product was verified for each of the acid, GSH, ceric ammonium nitrate. According to Table 4, The optimal sequence for achieving the maximum absorbance is glutathione then ceric ammonium nitrate then HCl.

Table 4: Effects of adding sequences for GSH assay

the addition sequence	λ = 500nm	λ = 700nm	λ = 900nm
GSH + CAN + HCl	0.570	0.386	0.184
GSH + HCl + CAN	0.394	0.266	0.134
CAN + GSH + HCl	0.499	0.324	0.177
CAN + HCl + GSH	0.480	0.293	0.156

3-3-5 Effect of Time

Beside to addition sequence effect to the components, effect of temperature and type of acid used in GSH assay, the effect of time for formation of turbid solution remains so important. Various points between 1 and 60 minutes might be tested to see how time affected the absorbance, conditions apllied for this procedure were 0.01 M of ceric ammonium nitrate solution, with 0.005 M of GSH using three drops of concentrated HCl.

Table 5: The effect of time for formation of turbid solution.

Time (min)	λ = 500nm	λ = 700nm	λ = 900nm
1	0.527	0.167	0.087
3	0.644	0.174	0.099
5	0.599	0.168	0.092
10	0.522	0.160	0.088

15	0.628	0.169	0.098
30	0.669	0.329	0.143
60	0.650	0.216	0.133

3-4 Calibration curve for glutathione

Calibration curve for GSH was conducted for many trials in order to obtain the best one. During estimation of GSH in sera samples, the referenced (kit) method showed GSH concentration in $\mu g.mL^{-1}$ therefore calibration curve under the same optimum conditions was constructed. Figure(3) shows calibration curve of GSH in $\mu g.mL^{-1}$ where the points lie on the straight line ranged from 20 to 180 $\mu g.mL^{-1}$ with R^2 equal to 0.9988.

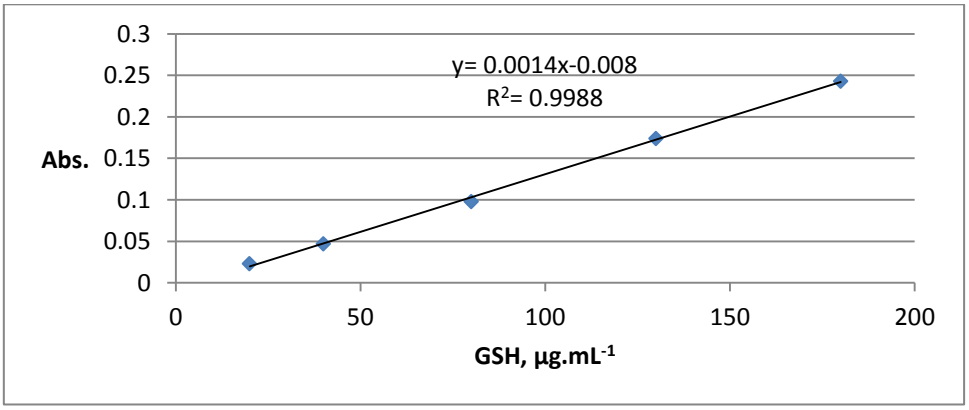

Figure (3): Calibration curve of GSH in $\mu g.mL^{-1}$ units.

3-5 Interferences

To illuminate the effect of the presence of sugars and amino acids as an interfering factor in glutathione estimation. A number of interferents including glucose, maltose, galactose, risbose, isoleucine, leucine, aspartic acid, valine, mannose, sucrose, methionine and bovine albumin were selected to study its effect.

Ceric ammonium nitrate 0.001 and 0.1 M

Table 6 shows effect of addition different interferents on GSH determination. The study was conducted at more than one concentration conditions.

Table 6: Effect of different interferents on glutathione determination

Interferent	With Ce(IV) (0.1M) %E	With Ce(IV) (0.001M) %E
Glucose	< 1.0	< 1.0
Maltose	< 1.0	< 1.0
Galactose	< 1.0	< 1.0
Risbose	< 1.0	< 1.0
Isoleucine	< 1.0	< 1.0
Leucine	Precipitate formation	< 1.0
Aspartic acid	< 1.0	< 1.0
Valine	< 1.0	< 1.0
Methanine	< 1.0	< 1.0
Mannose	< 1.0	< 1.0
Secrose	< 1.0	< 1.0
Bovine albumin	Precipitate formation	< 1.0

3-6 Estimation of serum glutathione in real participants samples

Sera samples were examined to determine the glutathione content in order to examine the validity of the existing method.

Some experiments were done with the deproteinization applied incorrectly. the results of these procedures caused unacceptable data.

Volume of 1mL of serum was taken and deproteinaztion achieved by using organic solvents method. Therefore, ethanol was used for this purpose.

First experiment

Volume of 1mL of serum was taken and deproteinizated using 1mL of ethanol then the mixture was centrifuged for 10min at 4000 rpm. After that 1.25 mL of the supernatant was mixed with 1.25 mL of 0.01M ceric ammonium nitrate solution (prepared through dissolving 0.1370 g of CAN in 25mL of distilled water) and 2

drops of conc. HCl. After 5min of mixing the first absorbance was measured at 500 and 900 nm. Then the same mixture was diluted again with 1 mL of distilled water and measure the second absorbance. Also, the same mixture was diluted again using 1 mL of distilled water and measure the third absorbance, so the final dilution of this mixture is made by 2 mL of distilled water. The absorbance was found to be very high and not compatible with the true value.

Table 7: Results of First experiment

Serum no.	Current method		referenced method Abs
	λ = 500	λ = 900	
1	1.628	0.722	0.034
1 (Diluted with 1mL distilled water)	1.312	0.500	
1(Diluted with 2mL distilled water)	1.021	0.375	
2	1.351	0.554	0.086
2(Diluted with 1mL distilled water)	0.958	0.336	
2(Diluted with 2mL distilled water)	0.674	0.230	
3	1.292	0.550	0.0799
3(Diluted with 1mL distilled water)	0.862	0.329	
3(Diluted with 2mL distilled water)	0.613	0.195	
4	1.305	0.500	0.0988
4(Diluted with 1mL distilled water)	0.911	0.318	
4(Diluted with 2mL distilled water)	0.633	0.210	
5	1.240	0.468	0.0724
5(Diluted with 1mL distilled water)	0.860	0.289	
5(Diluted with 2mL distilled water)	0.634	0.195	
6	1.408	0.542	0.1008
6(Diluted with 1mL distilled water)	0.962	0.343	
6(Diluted with 2mL distilled water)	0.703	0.237	

Second experiment

The same as the previous experiment, but only the volume of serum taken is replaced from 1 to 0.5mL. The absorbance was still found to have a high value in relation to the actual absorbance.

Volume of 0.5 mL of serum was taken and deproteinizated using 1mL of ethanol then the mixture was centrifuged for 10min at 4000 rpm. After that 1.25 mL of the supernatant was mixed with 1.25 mL of 0.01M ceric ammonium nitrate solution (prepared through dissolving 0.1370 g of Ce(IV) in 25mL of distilled water) and 2 drops of conc. HCl. After 5min of mixing the first absorbance was measured at 500

and 900 nm. Then the same mixture was diluted again with 1 mL of distilled water and measure the second absorbance. Also, the same mixture was diluted again using 1 mL of distilled water and measure the third absorbance, so the final dilution of this mixture is made by 2 mL of distilled water. The absorbance was still found to have a high value in relation to the actual absorbance.

Table 8: Results of Second experiment

Serum no.	Current method		referenced method Abs
	λ = 500	λ = 900	
1	2.155	1.260	0.0799
1 (Diluted with 1mL distilled water)	1.722	0.758	
1(Diluted with 2mL distilled water)	1.200	0.473	

Third experiment

The same as the first experiment, but only the volume of serum taken is replaced from 1 to 0.5 mL and the volume of ethanol taken is replaced from 1 to 2 mL. It was found that the absorption is still not compatible with the actual absorption.

Table 9: Results of third experiment

Serum no.	Current method		referenced method Abs
	λ = 500	λ = 900	
1	1.326	0.680	0.0988
1 (Diluted with 1mL distilled water)	1.100	0.426	
1(Diluted with 2mL distilled water)	0.800	0.310	

Fourth experiment

Volume of 0.25 mL of serum was taken and deproteinizated using 2mL of ethanol then the mixture was centrifuged for 10min at 4000 rpm.

After that

A. 0.25 mL of the supernatant was diluted with 1.5 mL of distilled water. Then 1.5 mL of from the previous solution was mixed with 1.5 mL of 0.01 M ceric ammonium nitrate solution (prepared through dissolving 0.1370 g of CAN in 25mL of distilled water) and 2 drops of conc. HCl. After 5min of mixing the first absorbance was measured at 500 and 900 nm.

B. 0.5 mL of the supernatant was diluted with 1.5 mL of distilled water. Then 1.5 mL of from the previous solution was mixed with 1.5 mL of 0.01 M ceric ammonium nitrate solution (prepared through dissolving 0.1370 g of CAN in 25mL of distilled water) and 2 drops of conc. HCl. After 5min of mixing the first absorbance was measured at 500 and 900 nm.

C. 1 mL of the supernatant was diluted with 1.5 mL of distilled water. Then 1.5 mL of from the previous solution was mixed with 1.5 mL of 0.01 M ceric ammonium nitrate solution (prepared through dissolving 0.1370 g of CAN in 25mL of distilled water) and 2 drops of conc. HCl. After 5min of mixing the first absorbance was measured at 500 and 900 nm.

Table 10: Results of Fourth experiment

Serum no.	the supernatant volume (mL)	Current method		referenced method
		λ = 500	λ = 900	
1	0.25	0.026	0.010	0.1047
	0.5	0.113	0.034	
	1	0.127	0.038	
2	0.25	0.144	0.045	0.0702
	0.5	0.124	0.039	
	1	0.126	0.034	

Volume of 0.25 mL of serum was taken and deproteinizated using 2mL of ethanol then the mixture was centrifuged for 10min at 4000 rpm.

After that 0.25 mL of the supernatant was diluted with 1.5 mL of distilled water. Then 1.5 mL of from the previous solution was mixed with 1.5 mL of 0.01 M ceric ammonium nitrate solution (prepared through dissolving 0.2741 g of CAN in 50 mL of distilled water) and 2 drops of conc. HCl. After 5min of mixing the first absorbance was measured at 900 nm.

Table 11: Glutathione estimation using ethanol for deproteinzation in real (serum) sample.

Serum no.	Referenced method µg.mL^{-1}	Current method µg.mL^{-1}
1	23.57143	20.678
2	16.42857	9.919
3	19.28571	14.6664
4	28.57143	22.3488
5	105.7143	44.0971
6	15	20.4806
7	25	23.3661
8	15	19.6309
9	20	20.485
10	17.14286	23.4632
11	30.71429	38.7213
12	14.28571	15.2679
13	17.85714	12.7686
14	16.42857	13.9448
15	19.28571	42.4849
16	10.71429	14.8252
17	302.8571	17.6154

18	17.85714	22.400
19	16.42857	18.0308
20	68.577	23.7218
21	15.71429	17.9089
22	40.71429	21.8434
23	49.28571	45.2666
24	31.42857	19.4818
25	45	26.6632
26	17.14286	20.9155
27	25	19.2415
28	27.14286	19.4067
29	42.85714	34.4302
30	22.14286	34.3831
31	25.71429	14.8055
32	40.71429	24.3275
33	100.7143	18.4805
34	32.85714	23.7865
35	32.14286	12.4987
36	12.14286	25.1937

37	20	37.5455
38	55	20.3811
39	26.42857	24.6702
40	22.85714	23.5177
41	19.28571	20.1981
42	11.42857	21.9307
43	27.14286	28.0726
44	118.5714	16.394
45	27.14286	15.6667
46	27.14286	54.4633
47	22.85714	17.597
48	13.57143	24.1176
49	27.14286	19.823
50	12.14286	16.9139
51	10	20.061
52	52.85714	30.9616
53	32.85714	17.6584
54	21.42857	44.0681
55	17.85714	61.0075

56	**10.71429**	**23.8911**
57	**78.57143**	**36.0387**
58	**12.14286**	**24.3691**
59	**12.85714**	**30.8122**
60	**37.85714**	**18.664**
61	**33.57143**	**35.2773**
62	**16.42857**	**35.1338**
63	**17.14286**	**23.1543**

3-7 Analytical performance studies

The accuracy of the method represented by the recovery (%Re) the relative error (%E), Precision of the method expressed as standard deviation and percent relative standard deviation (% RSD) was calculated by measuring the absorbance at different concentrations (0.001 and 0.009M) for 10 measurements for each concentration and the results are summarized in Tables 12 and 13.

Further analytical parameters were presented in table 14 and 15.

Table 12: Results of the current method at a concentration of 0.009 M

Exp.	Absorbance (X_i)	Mean deviation ($X_i - \overline{X}$)	Square deviation ($X_i - \overline{X}$)^2
1	0.229	-0.0243	0.00059049
2	0.261	0.0077	0.00005929
3	0.266	0.0127	0.00016129
4	0.231	-0.0223	0.00049729
5	0.248	-0.0053	0.00002809

6	0.268	0.0147	0.00021609
7	0.253	-0.0003	0.00000009
8	0.259	0.0057	0.00003249
9	0.275	0.0217	0.00047089
10	0.243	-0.0103	0.00010609
	ΣX=2.533		$\Sigma(X_i - \overline{X})^2 = 0.0021621$
	$\overline{X} = 0.2533$		

Table 13: Results of the current method at a concentration of 0.001M

Exp.	Absorbance (X_i)	Mean deviation ($X_i - \overline{X}$)	Square deviation ($X_i - \overline{X}$)^2
1	0.457	-0.1815	0.032942
2	0.477	-0.1615	0.026082
3	0.600	-0.0385	0.001482
4	0.672	0.0335	0.001122
5	0.731	0.0925	0.008556
6	0.671	0.0325	0.001056
7	0.701	0.0625	0.003906
8	0.674	0.0355	0.00126
9	0.731	0.0925	0.008556
10	0.671	0.0325	0.001056
	ΣXi=6.385		$\Sigma(X_i - \overline{X})^2 = 0.086021$
	$\overline{X} = 0.6385$		

$\overline{X} = \frac{\Sigma Xi}{n}$ …….. (3-1) n = number of measurements

$SD = \frac{\sqrt{\Sigma(Xi - \overline{X})^2}}{n-1}$ …….. (3-2) SD = Standard deviation

Then the percent relative standard deviation RSD% value was calculated from the following equation:

$RSD\% = \frac{S.D}{\overline{X}} \times 100\%$ …….. (3-3)

the relative error (% E) and the recovery ratio (% Re) were calculated from the following equation:

$\%E = \frac{d}{\mu} \times 100$ …….. (3-4) μ = True value

d= Difference true and analytical value

% Re = 100 ± % E …… (3-5)

The Limit of Detection (LOD) and Limit of Quantitation (LOQ) of the method were calculated from the following equation:

LOD = (3×SD/slope) …….. (3-6)

LOQ = (10× SD/slope) …….. (3-7)

Table 14: Results of the compatibility of the analytical method of the glutathione at a concentration of (0.005 and 0.009 M)

Parameter	Conc., 0.001M	Conc., 0.009M
Wavelength, nm	900	900
ΣXi	6.385	2.533
$\overline{X}$	0.6385	0.2533
$\Sigma(X_i - \overline{X})^2$	0.086021	0.0021621
SD	0.032588	0.00516648
RSD%	5.10386	2.03967

Table 15: Figures of merit of the current study

Parameter	0.001 M
Analytical Value	0.0013,0.0034,0.005
True value = μ	0.0015,0.003,0.0045
Absolute error (d)	-0.0002,0.0004,0.0005
% E_{rel}	-0.13, 0.13, 0.11
% Re	99.87, 100.13, 100.11
Correlation coefficient R	0.9993(0.9994)
Determination Coefficient, R^2	0.9986(0.9988)
Slope	34.284(0.0014)
Intercept	0.0025(-0.008)
LOD, $mol.Lit^{-1}$ ($\mu g.mL^{-1}$)	0.0002(3.43)
LOK, $mol.Lit^{-1}$ ($\mu g.mL^{-1}$)	0.0005(11.43)

Conclusions

The method based on turbidity through measuring at a novel near-infrared wavelength was found selective for detection of glutathione in sera samples. The current method is not affected by amino acids and sugars. It was fast, inexpensive, precise, sensitive and easily achieved. The presented procedure is applicable. However, in order to achieve this requirement, it is necessary to rely on the regression equation. Further, estimation of glutathione, at the optimized current conditions, could be conducted by using turbidimeter instead of spectrophotometer.

References

[1] Al-Temimi AA, Al-Mossawi A-E-B, Al-Hilifi SA, Korma SA, Esatbeyoglu T, Rocha JM, et al. Glutathione for food and health applications with emphasis on extraction, identification, and quantification methods: A review. Metabolites. 2023;13(4):465.

[2] Umansky C, Morellato AE, Rieckher M, Scheidegger MA, Martinefski MR, Fernández GA, et al. Endogenous formaldehyde scavenges cellular glutathione resulting in redox disruption and cytotoxicity. Nat Commun. 2022;13(1):745.

[3] Moscoso FG, Queirós C, González P, Lopes-Costa T, Silva AMG, Pedrosa JM. Selective Determination of Glutathione Using a Highly Emissive Fluorescent Probe Based on a Pyrrolidine-Fused Chlorin. Molecules. 2023;28(2):568.

[4] Jana A, Joseph MM, Munan S, Shamna K, Maiti KK, Samanta A. A single benzene fluorescent probe for efficient formaldehyde sensing in living cells using glutathione as an amplifier. J Photochem Photobiol B Biol. 2021;214:112091.

[5] Shuhua X, Ziyou L, Ling Y, Fei W, Sun G. A role of fluoride on free radical generation and oxidative stress in BV-2 microglia cells. Mediators Inflamm. 2012;2012.

[6] Lin J, Xie J, Luo L, Gänzle M. Characterization of GshAB of Tetragenococcus halophilus: a two-domain glutathione synthetase. Appl Microbiol Biotechnol. 2023;107(9):2997–3008.

[7] Lu SC. Dysregulation of glutathione synthesis in liver disease. Liver Res. 2020;4(2):64–73.

[8] Nuhu F, Gordon A, Sturmey R, Seymour A-M, Bhandari S. Measurement of glutathione as a tool for oxidative stress studies by high performance liquid chromatography. Molecules. 2020;25(18):4196.

[9] Penninckx MJ, Elskens MT. Metabolism and functions of glutathione in micro-organisms. Adv Microb Physiol. 1993;34:239–301.

[10] Bachhawat AK, Kaur A. Glutathione degradation. Antioxid Redox Signal. 2017;27(15):1200–16.

[11] 11. Bartolini D, Stabile AM, Bastianelli S, Giustarini D, Pierucci S, Busti C, et al. SARS-CoV2 infection impairs the metabolism and redox function of cellular glutathione. Redox Biol. 2021;45:102041.

[12] Giustarini D, Milzani A, Dalle-Donne I, Rossi R. How to Increase Cellular Glutathione. Antioxidants. 2023;12(5):1094.

[13] Giustarini D, Dalle-Donne I, Tsikas D, Rossi R. Oxidative stress

and human diseases: origin, link, measurement, mechanisms, and biomarkers. Crit Rev Clin Lab Sci. 2009;46(5–6):241–81.

[14] Ballatori N, Krance SM, Notenboom S, Shi S, Tieu K, Hammond CL. Glutathione dysregulation and the etiology and progression of human diseases. 2009;

[15] Hayes JD, Dinkova-Kostova AT, Tew KD. Oxidative stress in cancer. Cancer Cell. 2020;38(2):167–97.

[16] Giustarini D, Fanti P, Matteucci E, Rossi R. Micro-method for the determination of glutathione in human blood. J Chromatogr B. 2014;964:191–4.

[17] Hu L, Ju M, Gao A, Chen H, Hou A. A supersensitive fluorescent probe for biothiols by regulating the click reaction and its application in glutathione detection in food samples. Dye Pigment. 2022;200:110164.

[18] Li G, Ma W, Yang Y, Zhong C, Huang H, Ouyang D, et al. Nanoscale covalent organic frameworks with donor–acceptor structures as highly efficient light-responsive oxidase-like mimics for colorimetric detection of glutathione. ACS Appl Mater Interfaces. 2021;13(41):49482–9.

[19] Yin Y, Zhen B, Sun J, Ouyang J, Na N. Detection of glutathione, cysteine, and homocysteine by online derivatization-based electrospray mass spectrometry. Rapid Commun Mass Spectrom. 2022;36(11):e9291.

[20] Habib A, Mabrouk MM, Fekry M, Mansour FR. Glycerol as a new mobile phase modifier for green liquid chromatographic determination of ascorbic acid and glutathione in pharmaceutical tablets. J Pharm Biomed Anal. 2022;219:114870.